International Journal of Hydrogen Energy 193 (2025) 152367

Contents lists available at ScienceDirect

International Journal of Hydrogen Energy

journal homepage: www.elsevier.com/locate/he

Failure mechanisms of onboard hydrogen storage systems under real-world road-induced vibrations

Tao Zhang [a,b], Zhijie Duan [c,d], Feiyang Liu [a,e], Weijie Yang [a,b,*]

[a] Department of Power Engineering, North China Electric Power University, Baoding, 071003, Hebei, China
[b] Hebei Key Laboratory of Energy Storage and Integrated Energy Systems, North China Electric Power University, Baoding, 071003, Hebei, China
[c] To High Hydrogen Testing (Baoding) Co., LTD, Hebei, China
[d] Tianjin University, Jinnan, 300354, Tianjin, China
[e] Huaneng Anyuan Power Plant, Pingxiang, 337200, Jiangxi, China

ARTICLE INFO

Keywords:
Onboard hydrogen storage system
Structural failure
Modal analysis
Random vibration analysis
Failure mechanisms

ABSTRACT

Onboard hydrogen storage systems play a pivotal role in hydrogen fuel cell vehicles, and their structural integrity is directly linked to vehicle safety. Owing to their high sensitivity to vibrations, these systems are susceptible to resonance and fatigue under complex and dynamic road conditions, potentially resulting in structural failure and safety risks. While prior studies have primarily focused on strength validation under standard road scenarios, there remains a lack of comprehensive investigation into the multi-dimensional vibration-induced failure mechanisms across various vehicle types in real-world environments. In this study, we examine the onboard hydrogen storage systems of both commercial and passenger vehicles through modal analysis to determine resonance frequencies, integrated with real-world road spectrum data and random vibration theory. Simulations were conducted under twelve representative road conditions. The results reveal that critical stress concentration zones appear under road conditions 6 and 4 for commercial and passenger vehicles, respectively, with maximum equivalent stresses reaching 134.77 MPa and 344.45 MPa. Furthermore, structural deformations and fractures were observed in the cylinder saddles and brackets, leading to loosening, collapse, and potential cylinder detachment. Resonance and high-frequency vibrations were identified as the primary causes of these failures. This work provides valuable insights into the failure modes and mechanisms of hydrogen storage systems under complex vibration environments, offering theoretical guidance and empirical data for their structural optimization and safety design.

1. Introduction

As the global energy structure transforms and sustainable development advances, hydrogen energy has gained widespread attention as a clean and environmentally friendly energy source. To enable the widespread application of hydrogen energy, hydrogen storage technology has become a critical component. Among various methods, high-pressure gaseous hydrogen storage is widely used in the transportation sector due to its technological maturity and advantages such as fast hydrogen filling and release. Especially in hydrogen fuel cell vehicles, the technology has become the mainstream choice for onboard hydrogen storage systems. However, the onboard hydrogen storage system, a core component of hydrogen fuel cell vehicles, plays a crucial role in storing and supplying hydrogen, as well as supporting key components. A failure could lead to serious consequences, potentially jeopardizing both vehicle safety and user life [1,2].

Therefore, the design, optimization, and failure prevention of onboard hydrogen storage systems have been important research areas in both academia and engineering. Currently, research on hydrogen storage systems has made certain progress, particularly in areas such as hydrogen fueling-induced temperature rise and component failures. Yan-Lei Liu, Liang Wang, M. Cristina Galassi et al. [3–5] studied the temperature rise distribution, refueling rate, initial pressure, and the effect of hydrogen precooling during the rapid hydrogen charging process of hydrogen storage tanks. They concluded that the refueling rate and pressure have a significant impact on temperature rise, and that precooling technology can effectively reduce temperature rise, ensuring safe refueling. Research on hydrogen refueling temperature rise

* Corresponding author. Department of Power Engineering, North China Electric Power University, Baoding, 071003, Hebei, China.
E-mail address: yangwj@ncepu.edu.cn (W. Yang).

https://doi.org/10.1016/j.ijhydene.2025.152367
Received 15 April 2025; Received in revised form 25 October 2025; Accepted 31 October 2025

indicates that factors such as refueling rate, pressure, hydrogen pre-cooling, and materials have a significant impact on the temperature rise of hydrogen storage tanks. Optimizing refueling strategies and pre-cooling technologies can effectively control temperature rise, improving refueling efficiency and safety. Wei Zhou, Yikai Zhang et al. [6,7] conducted a study on the failure analysis and optimization design of hydrogen storage containers. They concluded that design factors significantly affect the container strength, durability, and fatigue life, and that optimized design can improve the container safety. Research on structural failure indicates that the fatigue failure of composite hydrogen tanks is influenced by factors such as temperature loading, porosity, and design considerations. Optimizing the design, improving stress distribution during the refueling process can significantly enhance the tank durability and safety. Additionally, different design parameters have a critical impact on the tank fatigue life and burst pressure. However, there is relatively little research on the overall vibration failure of onboard hydrogen storage systems, which hinders further structural optimization of the storage system and the development of appropriate failure prevention measures.

Therefore, to further advance the research on vibration failure of onboard hydrogen storage systems, this paper is based on the research findings related to mechanical system failure and focuses on vibration failure analysis to examine the vibration response under different system conditions. Based on a literature review, it was found that significant progress has been made in the research related to system vibration failure, vibration assessment, vibration analysis, and vibration control. Liu et al. [8] studied the high-frequency vibration fatigue issues of subway vehicle bumpers through field tests and numerical simulations. Wu et al. [9] used numerical simulations to analyze the high-frequency vibration fatigue of antenna beams. Lee et al. [10] assessed the safety of hydrogen storage containers by combining numerical models with fatigue analysis. All concluded that structural optimization could significantly improve reliability. Lei et al. [11] established a new method for vibration damage assessment from the perspectives of signal modulation using amplitude-phase modulation. Kinoshita et al. [12] developed a similar approach from the energy perspective by establishing a basic energy equation. Manouchehrynia et al. [13] employed frequency-domain analysis, and Chen et al. [14] combined experimental and finite element methods, both focusing on specific components to develop high-precision life assessment models. Wang et al. [15] conducted vibration studies of bridges induced by vehicle deceleration using coupled vibration analysis and proposed an efficient modeling method to reduce computational costs. Zhang et al. [16] used finite element methods for random vibration modeling of magnetic levitation vehicle systems, analyzing vibration characteristics under different operating conditions. You et al. [17] used the pseudo-excitation method to study axle box uncoupling vibration fatigue, validating the effectiveness of the synthesized power spectral density (PSD) spectrum. Wang et al. [18] and Aathif Akmal et al. [19] respectively studied the vibration damping of slender beam systems and the damping characteristics of engine mounting materials, finding that vibration damping efficiency can be significantly improved by optimizing system design parameters or selecting suitable materials.

Currently, significant progress has been made in vibration-related research on mechanical system vibration fatigue, vibration characteristics, and their impact on structural stability. Appropriate optimization designs and vibration reduction measures have been proposed for applications in different fields. However, most studies focus on the failure evaluation of a single vibration type or specific components. Research on vibration failure of onboard hydrogen storage systems primarily concentrates on explaining failure phenomena and verifying structural strength under normal road conditions. There is a lack of analysis on the vibration failure modes and mechanisms of onboard hydrogen storage systems under complex road conditions, based on real vehicles and in multiple dimensions, across different vehicle types.

Therefore, this study conducted real-world road spectrum acquisition experiments to capture multi-dimensional acceleration signals across 12 distinct road conditions, enabling stochastic vibration simulations of hydrogen storage systems under various operational scenarios. Based on the 3σ theory, the stress and strain values of the system were calculated, and corresponding failure modes were analyzed to reveal the underlying failure mechanisms. The results indicate that the stress concentration points of the hydrogen storage systems in commercial and passenger vehicles occur at road conditions 6 and 4, with maximum equivalent stresses of 134.77 MPa and 344.45 MPa, respectively. Additionally, the cylinder saddle and bracket were prone to deformation and fracture, resulting in loosened connections, structural collapse, and hydrogen cylinder detachment. Resonance and high-frequency vibrations were identified as the primary causes of failure. This research establishes a theoretical foundation for the safety design and failure prevention of hydrogen-powered vehicles, with significant implications for their commercial deployment and public safety assurance.

2. Method

2.1. Modal analysis theory

Modal analysis can reveal the dynamic characteristics of the system, such as natural frequencies, vibration patterns, and damping ratios, which form the foundation of random vibration analysis. Among these parameters, natural frequencies correspond to the specific frequencies at which a linear n-degree-of-freedom system exhibits free vibration, while mode shapes represent the characteristic displacement patterns associated with each natural frequency. The acquisition of natural frequencies and mode shapes provides a foundational basis for assessing resonance phenomena within the system.

This technique enables the decoupling of complex multi-degree-of-freedom systems into simplified single-degree-of-freedom systems, significantly streamlining the calculation process. Additionally, it not only helps identify dominant modes and clarify the primary response characteristics of the systems, but also provides essential data support for PSD calculations [20] and resonance risk assessment, laying the groundwork for failure mechanism research. Therefore, performing modal analysis before conducting random vibration analysis can simplify the research process, improve computational efficiency, and facilitate the analysis and interpretation of random vibration problems [21,22].

Assuming the structural stiffness of the onboard hydrogen storage system is constant and unaffected by external forces [23,24], the dynamic differential equation of the system is:

$$[M]\{\ddot{x}\}+[C]\{\dot{x}\}+[K]\{x\}=0 \tag{1}$$

where $[M]$ is the mass matrix, $[C]$ is the damping matrix, $[K]$ is the stiffness matrix.

According to previous research, Tsai, T-Y et al. [25] omitted damping in their analysis of the response spectrum of single-degree-of-freedom systems. Liang, W et al. [26] similarly disregarded damping when evaluating the dynamic response of oscillators to underwater shock waves.

Based on the established analysis methods commonly found in the literature, the system is analyzed by using a damping-free model. The calculation process is simplified without affecting the analysis of the results, leading to the following simplified differential equation:

$$[M]\{\ddot{x}\}+[K]\{x\}=0 \tag{2}$$

The structural displacement can be decomposed into the superposition of simple harmonic motions, so the displacement array can be expressed as:

$$\{x\}=\{A\}\sin(\omega t+\varphi) \tag{3}$$

where $\{x\}$ is the non-zero amplitude array, ω is the angular frequency, and φ is the initial phase angle.

Substituting Equation (3) into Equation (2) yields:

$$([K]-\omega^2[M])\{A\}=\{0\} \tag{4}$$

Based on the principles of linear algebra, if the array $\{A\}$ is not entirely zero, the determinant within the brackets on the left side must equal zero. This allows us to solve the eigenvalues and their corresponding eigenvectors.

2.2. Random vibration analysis theory

The frequency response function (FRF) [27] is the key to describing the dynamic characteristics of a system in the frequency domain, which reflects the intrinsic properties of the system and is related to the mass, stiffness, and damping of the system. This function can characterize the amplitude amplification or attenuation of the system output to the input at different frequencies and the change of phase. More significantly, FRF analysis facilitates analysis of resonance frequencies, dynamic response characteristics, and vibrational behavior. As a vital tool in random vibration analysis, it provides an indispensable theoretical foundation for investigating the dynamic performance of onboard hydrogen storage systems and guiding structural design optimization [28,29].

This work simulates random vibration under constant ambient temperature conditions. As indicated by de Miguel N et al. [30], when the hydrogen storage tank is continuously discharged to approximately 20 % state of charge (SOC), the temperature of the vehicle's hydrogen storage system will be at least 20 °C lower than the ambient temperature upon arrival at the refueling station. A temperature span of this magnitude is considered insufficient to significantly affect the material properties or stress distribution of system components. Therefore, the influence of temperature variations during normal operation of the onboard hydrogen storage system is disregarded in this analysis.

In practical engineering, to describe the amplitude and frequency of the response, the frequency response function is typically expressed in complex form, as shown in the following equation:

$$H(\omega)=A(\omega)-iB(\omega) \tag{5}$$

Where the amplitude of the frequency response function equals the ratio of the output amplitude to the input amplitude of the system, and the ratio of the imaginary part to the real part of the frequency response function equals the tangent of the phase angle, as shown in Equations (6) and (7):

$$|H(\omega)|=\sqrt{A^2+B^2}=\frac{a_{out}}{a_{in}} \tag{6}$$

Where a_{out} is the single-degree-of-freedom output and a_{in} is the single-degree-of-freedom input.

$$\frac{\mathrm{Im}[H(\omega)]}{\mathrm{Re}[H(\omega)]}=\frac{B}{A}=\tan\phi \tag{7}$$

When a single power spectral density value is input into the system, the system output $S_{out}(\omega)$ is as shown in Equation (8) [31,32]:

$$S_{out}(\omega)=|H(\omega)|^2 S_{in}(\omega) \tag{8}$$

Where S_{out} is the power spectral density response, S_{in} is the power spectral density input, and the value comes from the input PSD.

In random vibration simulations accounting for inherent uncertainties, the average response of the system is taken as the simulation result, i.e, it is used to analyze the response result of the system by calculating its root mean square (RMS) value. The RMS is the time-averaged square response which can be used to quantify the energy magnitude of a random vibration, describing the degree of concentration of the mean value of its random variable. As demonstrated in Equation (9), elevated RMS values correspond to increased energy input to the system, manifesting as enhanced vibrational frequencies and amplitude characteristics.

$$RMS=\sqrt{\int_0^\infty S(\omega)d\omega} \tag{9}$$

Random vibration analysis is fundamentally grounded in the 3σ principle, requiring both input and output parameters to adhere to specific probabilistic distributions, where external random excitations and system responses conform to Gaussian normal distributions [33], as illustrated in Fig. 1. The output responses (including displacement, stress, and strain) exhibit statistically defined probability distributions: 68.3 % within ±1σ, 95.4 % within ±2σ, and 99.7 % within ±3σ ranges. Therefore, since there is only a 0.3 % probability that the response result exceeds the 3σ range in practical applications, random vibration simulations adopt the 3σ value as the final computational result.

We employ the von Mises equivalent stress criterion, which is theoretically well-suited for analyzing yield failure in mechanical components. The criterion comprehensively considers the combined effects of the three principal stresses, thereby overcoming the limitations of traditional theories that rely on a single stress component. It provides a reliable basis for predicting material yield behavior under complex loading conditions and for determining whether a structure remains in a safe state. In addition, the applicability of this criterion has also been demonstrated in prior studies. For instance, Li et al. [34] applied it to analyze fatigue failure in feedwater heating tubes, estimating damage progression and remaining service life, while Abdullah et al. [35] employed it to evaluate the initiation of fatigue cracks on the inner surface of helical springs.

2.3. Finite element model

To study the response characteristics of commercial and passenger vehicle onboard hydrogen storage systems under random vibration excitations from different road conditions and to evaluate their safety in complex scenarios, the study focuses on two representative configurations: an 8-cylinder commercial vehicle onboard hydrogen storage system and a 2-cylinder passenger vehicle onboard hydrogen storage system. The 8-cylinder commercial vehicle onboard hydrogen storage system contains components such as cylinder valves, pressure relief valves, pipelines, and connectors. However, these parts increase computational complexity and reduce efficiency. Therefore, they were removed without significantly affecting the simulation results. The 2-cylinder passenger vehicle onboard hydrogen storage system consists of a front hydrogen cylinder system and a rear hydrogen cylinder system. Since the structures of the front and rear systems are similar, we selected the rear hydrogen cylinder system as the main analysis object. The above simplification methods for the model help us reduce simulation computation while ensuring the research results maintain high

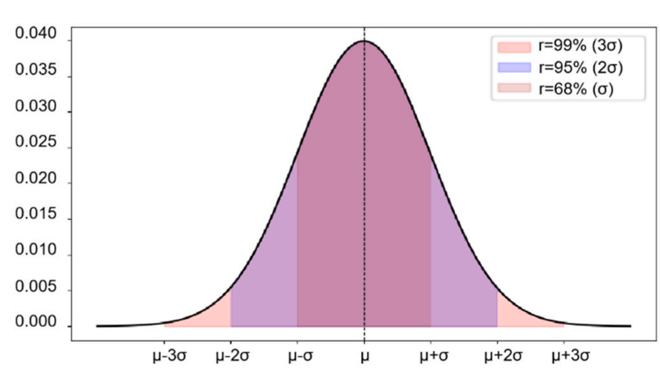

Fig. 1. Gaussian normal distribution curve.

representativeness and practical significance. The simplified finite element model [36] is presented in Fig. 2.

During random vibration analysis, the components of the onboard hydrogen storage system are connected by bonded contacts. Therefore, the system does not experience significant separation or deformation between components under intense vibration loads. The materials and physical properties of each component are listed as Table 1.

The data in Table 1 is taken from “Impact Vibration Analysis of Hydrogen Supply Systems for Fuel Cell Vehicles and Research on Framework Size Optimization [37].”

2.4. Simulation condition settings

In passenger vehicles, hydrogen storage cylinders are commonly integrated and secured to the underbody structure via front and rear mounting brackets, which incorporate cushion pads and bottle clamps. In contrast, commercial vehicles employ a rigid fixation method whereby the hydrogen cylinder assembly is directly mounted to the chassis frame using support saddles and high-strength lashing straps. Therefore, to accurately simulate an onboard hydrogen storage system being immobilized in a vehicle, fixed constraints were applied to: (i) the base plate of the commercial vehicle onboard hydrogen storage system (indicated by the blue surface in Fig. 3(a)), and (ii) the interface between the passenger vehicle onboard hydrogen storage system and vehicle chassis (shown in blue in Fig. 3(b)). To simplify the random vibration analysis process, the following assumptions were adopted for both hydrogen storage systems.

(1) The material is linear elastic and has constant physical properties, meaning its attributes do not change during the simulation process.
(2) The overall stiffness, damping, and stiffness matrix of the structure are constant values.
(3) The applied acceleration power spectral density and fixed constraint load do not vary with simulation.
(4) The damping force acting on the structure is much smaller than the inertial force and elastic force.
(5) The random vibration simulation does not vary with time, and the response is a stable random process.

3. Results and discussions

3.1. Modal analysis

Modal analysis [38] serves as an essential prerequisite for random vibration analysis, identifying structural natural frequencies, vibration patterns, and damping characteristics that provide critical parameters for dynamic response analysis. This analysis can effectively avoid the resonance matching between the intrinsic frequency of the onboard hydrogen storage system and the excitation frequency of the road surface, thereby mitigating potential structural damage. Furthermore, modal analysis simplifies multi-degree-of-freedom systems while improving computational accuracy, enabling easier acquisition of resonance frequencies and corresponding stresses and deformations for both passenger and commercial vehicle systems - key references for failure risk assessment [39]. The 12-order modal analysis results for these systems are presented in Tables 2 and 3. A resonance frequency bar graph is plotted for ease of observation and analysis, as shown in Fig. 4.

Table 1
Material parameters of onboard hydrogen storage system components.

component	material	Modulus of elasticity GPa	Poisson ratio	Density Kg/m^3
Hydrogen storage bottle	Aluminum inner liner + carbon drill dimension	210	0.3	1970
frame	6063Aluminum	69	0.33	2700
saddle	Aluminum Alloy	70	0.33	2720
bandage	stainless steel	193	0.3	7750
pin roll	45 Steel	200	0.3	7850
bolt and nut	35 Steel	195	0.3	7850

Analysis of Fig. 4 reveals significantly higher resonance frequencies in the passenger vehicle onboard hydrogen storage systems compared to the commercial vehicle onboard hydrogen storage systems, with both systems exhibiting frequency escalation proportional to modal order. Tabulated data (Tables 2 and 3) demonstrate substantially greater deformation magnitudes and displacement ranges in the passenger vehicle system. However, under high-frequency vibrational loading, these displacements exceed the stiffness threshold of the material, inducing potential structural compromise. When the system frequency reaches a higher resonance frequency, the deformation and strain of the system will increase significantly, exceeding the allowable deformation range of the material, which may lead to irrecoverable large deformation of the system, and ultimately cause damage and failure of the structure.

3.2. Signal acquisition and processing

3.2.1. Acceleration spectrum signal acquisition

This study focuses on analyzing the vibration characteristics of vehicle-mounted hydrogen storage systems under 12 representative road conditions. The research scope deliberately excludes the influence of vibration load duration on system behavior. In acquiring road profile signals, the primary objective is to assess the effects of different road-induced vibration loads on the system response, rather than the temporal length of loading.

For a given road condition, the vibration spectrum remains consistent regardless of the signal acquisition duration. Therefore, the acquisition time is selected solely to ensure that the data collected is sufficient to produce statistically meaningful results.

The road spectrum acquisition was conducted using TestLink software to capture triaxial vibration signals under 12 representative road conditions (including twist roads, bumpy roads, gravel roads A/B/C, cobblestone roads A/B, washboard roads A/B/C, short-wave, and long-

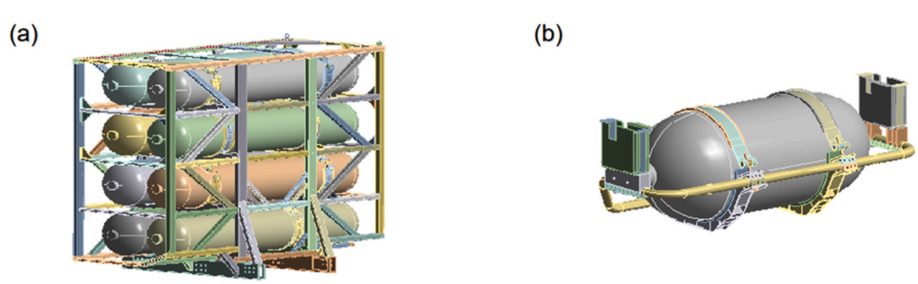

Fig. 2. Simplified finite element model of onboard hydrogen storage system:(a) **Commercial vehicle onboard hydrogen storage system, (b) Passenger vehicle onboard hydrogen storage system.**

Fig. 3. Fixed constraint application surface of the onboard hydrogen storage system: (a) **Commercial vehicle onboard hydrogen storage system, (b) Passenger vehicle onboard hydrogen storage system.**

Table 2
Mode analysis results of onboard hydrogen storage system of passenger vehicles.

Modal order of passenger cars	Frequency (Hz)	Maximum shape variable (mm)	Equivalent elastic strain
1	19.996	5.0482	4.2552×10^{-3}
2	26.905	6.4776	1.2247×10^{-2}
3	31.843	5.8039	1.251×10^{-2}
4	44.635	7.8238	1.3325×10^{-2}
5	45.28	6.4173	2.3313×10^{-2}
6	64.962	8.3222	3.2663×10^{-2}
7	70.546	25.348	2.6954×10^{-2}
8	73.964	24.132	2.4165×10^{-2}
9	84.841	28.854	3.4051×10^{-2}
10	88.558	31.57	4.3451×10^{-2}
11	109.55	154.65	0.13523
12	142.65	219.81	0.18542

Table 3
Mode analysis results of onboard hydrogen storage system for commercial vehicles.

Mode order of commercial vehicles	frequency (Hz)	Displacement deformation amount (mm)	Equivalent elastic strain
1	17.548	2.2802	4.8887×10^{-3}
2	18.284	1.9877	4.1901×10^{-3}
3	22.092	3.2391	2.2997×10^{-3}
4	42.668	2.2947	1.5717×10^{-2}
5	43.989	2.3262	1.7631×10^{-2}
6	46.334	2.84	1.0051×10^{-2}
7	54.90	2.5429	1.3719×10^{-2}
8	56.343	2.9231	1.0524×10^{-2}
9	59.439	3.6553	1.4097×10^{-2}
10	62.504	2.9141	1.2533×10^{-2}
11	64.457	3.2956	3.3186×10^{-2}
12	70.785	4.1649	2.0488×10^{-2}

wave roads), as illustrated in Fig. 5. The twelve road conditions selected cover a broad spectrum of scenarios that a vehicle may encounter during actual driving, while also encompassing the typical frequency range (0–100 Hz) that influences vehicle dynamic performance. This frequency band aligns with the range used by Zhang et al. [40] in their study on ride comfort and energy dissipation in vehicle suspension systems under non-stationary random road excitation.

According to previous research, Manouchehrynia R et al. [41] captured experimentally measured random road load strain data at a 500 Hz sampling rate over 60 s under three distinct road conditions, and proposed recommendations for determining fatigue life characteristics under such random strain conditions. Wang A et al. [42] performed finite element-based fatigue life predictions for rubber suspension bushings using load pulses extracted from a 232 s segment of the load spectrum. The road load data in this study were acquired over durations of 526 s for commercial vehicles and 738 s for passenger vehicles. These acquisition periods are deemed representative and universally applicable for the intended analytical purposes.

When plotting, we took the vertical axis 0 scale as the horizontal

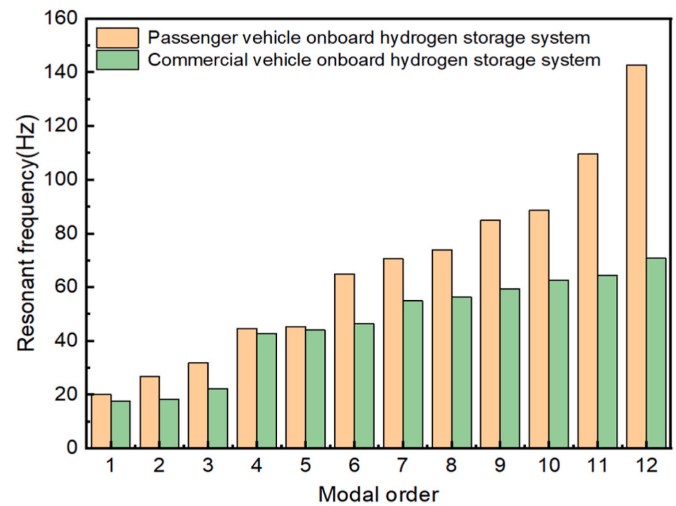

Fig. 4. Resonance frequency of modal analysis of onboard hydrogen storage system.

reference axis, then the farther away from the axis can indicate that the signal response is more sensitive, the larger the acceleration signal value. Comparative analysis reveals significantly stronger vibrational responses in passenger vehicles versus commercial vehicles (Fig. 5).

3.2.2. PSD signal conversion

The collected acceleration time-domain signals were processed through denoising, filtering, and detrending operations in MATLAB. Fourier transformation [43] was subsequently applied to convert the processed signals into power spectral density representations. However, since the power spectral density in the high-frequency band is close to 0, the PSD signals were intercepted within 100 Hz and 50 Hz for commercial vehicles and passenger cars, respectively (Fig. 6). These triaxially (X, Y, Z) acquired power spectral density signals from twelve road conditions served as vibrational excitation inputs for the random vibration analysis of the onboard hydrogen storage system.

The RMS value serves as an effective indicator of signal energy magnitude, enabling both preliminary assessment of vibration impact levels across various road conditions and evaluation of system safety and stability. The average signal power is quantified by calculating the RMS value, which can be obtained by performing a root-mean-square operation on the power spectral density that describes the energy distribution of the signal in the frequency domain during a random process. Fig. 7 presents a comparative visualization of these computed RMS values, illustrating triaxial (X, Y, Z) vibrational energy characteristics for both commercial and passenger vehicles under diverse road conditions.

Comparative analysis of the RMS values in Fig. 7(a) and (b) reveals significantly higher vibrational energy levels in the onboard hydrogen storage system of the passenger vehicle compared to that of the commercial vehicle system under identical road conditions. This observed disparity leads to three key conclusions.

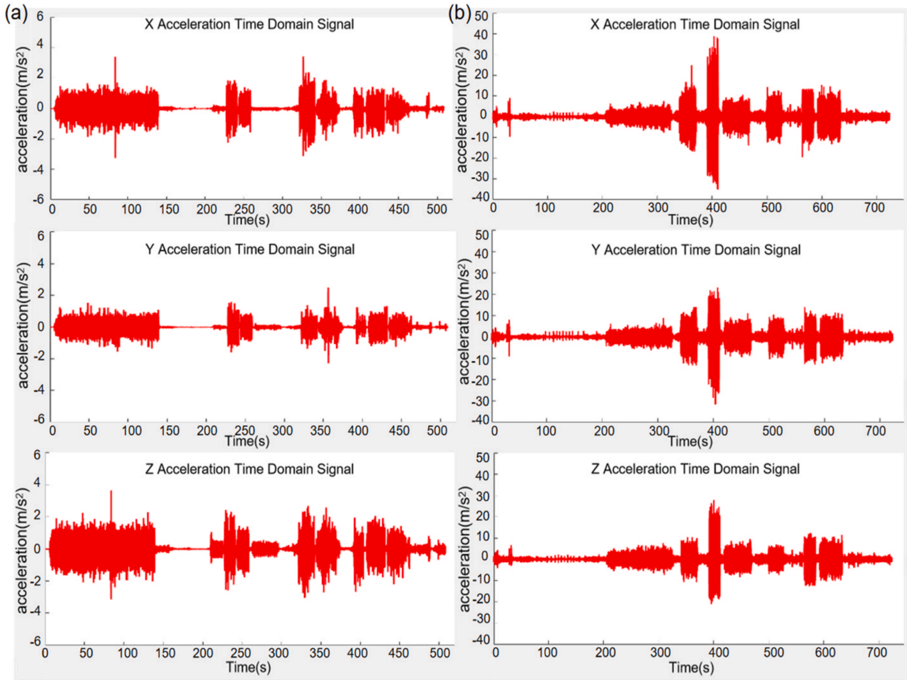

Fig. 5. Acceleration time domain signal of the onboard hydrogen storage system: (a) Acceleration time domain signal of the commercial vehicle onboard hydrogen storage system, (b) Acceleration time domain signal of the passenger vehicle onboard hydrogen storage system.

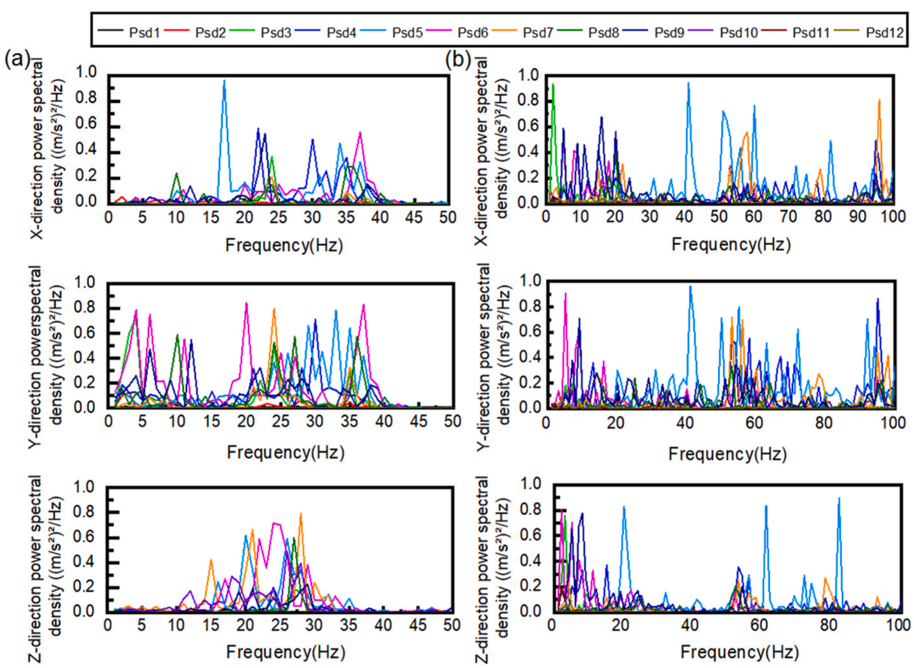

Fig. 6. PSD curve of onboard hydrogen storage system: (a) passenger vehicles, (b) commercial vehicles.

(1) Under identical road conditions, passenger vehicles exhibit significantly greater vibrational response amplitudes compared to commercial vehicles. The structural design differences between vehicle types - with passenger vehicles prioritizing lightweight construction for comfort versus commercial vehicles employing heavier designs for load capacity - correlate with this observed dynamic behavior.
(2) Comparative analysis reveals superior vibration attenuation characteristics in commercial vehicle hydrogen storage mounting systems. The cab-mounted configuration of the commercial vehicle demonstrates markedly higher vibration damping performance relative to the chassis-suspended system of the passenger vehicle.
(3) Road surface excitations propagate more efficiently through passenger vehicle systems. This effect coincides with the tire configuration differences: commercial vehicles' thick, high-load tires versus passenger vehicles' lightweight low-profile tires, resulting in more direct vibration transmission to the hydrogen storage system.

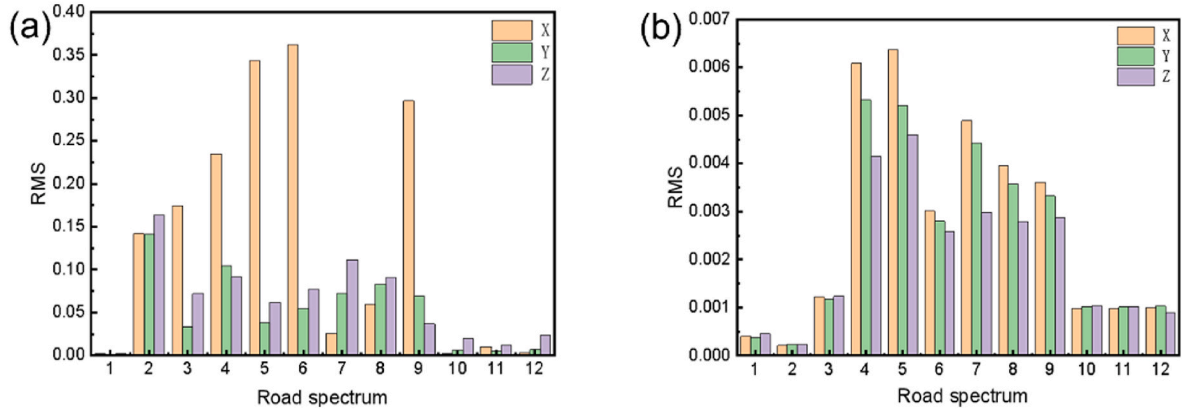

Fig. 7. Bar graph of PSD signal RMS value of onboard hydrogen storage system:(a) Commercial vehicle RMS value, (b) Passenger vehicle RMS value.

As demonstrated by the above conclusions, both measures—installing the onboard hydrogen storage system in the driver's compartment and equipping the vehicle with thicker, high-load tires—can effectively reduce vibration impacts from the road surface.

3.3. Vibration simulation and failure analysis

We analyzed the failure modes and characteristics of the system and assessed the extent of failure to determine its safety by observing the equivalent stress nephograms [44] of the onboard hydrogen storage system under random vibration. The equivalent stress nephogram in Fig. 8 reveals that the onboard hydrogen storage system of the commercial vehicle bears higher stress in the X and Y directions at the front and rear reinforcement brackets, the central bracket, and the fixed base of the frame. In the Z direction, higher stress is mainly located at the hydrogen cylinder saddle and the welded joints of the brackets. These areas are frequently and predominantly subjected to complex multiaxial loads, especially alternating stresses caused by vibration, and are prone to failure behaviors such as fractures or wear-induced cracking. When the system is in a frequent vibration environment, due to the stress concentration at the welded joints, these parts are prone to fatigue damage. In particular, if the connection between the hydrogen storage cylinder saddle and the bracket is not well-designed or of insufficient strength, then the dynamic loading may lead to loosening of the connection or structural damage, which may ultimately lead to the collapse of the system and affect the overall operation.

The equivalent stress distributions in the passenger vehicle onboard hydrogen storage system under X- and Z-direction vibrational loading are presented in Fig. 9(a) and (c). Stress maxima localize at two critical regions: (i) vehicle chassis mounts and bracket connections at both ends of the system, and (ii) cylinder saddle and strap to bracket connection. These stress concentrations may induce structural compromise through either support deformation or fracture initiation. Fig. 9(b) reveals the Y-direction vibrational stress distribution, demonstrating significant stress concentration at the cylindrical saddle seat which may lead to embrittlement of the saddle material and large structural deformations. There are two main reasons for the failure behavior described above: (i) the structural fragility inherent in the structure of the main load-bearing components of the bracing system, exacerbated by the continuous gravitational loading, and (ii) transverse vibration resulting in uneven force distribution across the saddle and concentrated stresses in thin-walled sections.

In summary, the structural integrity of the onboard hydrogen storage system can be enhanced through three design modifications: (i) increased thickness at stress concentration zones, (ii) reinforcement ribs in fracture-prone regions, and (iii) vibration-damping interfaces at saddle connections. These measures can enhance the buffering capacity of the saddle against vibration-induced pressure from the hydrogen storage cylinder, thereby reducing stress on the saddle and preventing its failure. The proposed optimization strategy ensures that the system has the potential to significantly improve vibration resistance while maintaining structural stability under operating conditions.

To analyze the impact of different road conditions on system failure severity, we summarized the maximum equivalent stresses and maximum deformations experienced by various types of onboard hydrogen storage systems under different acceleration power spectral densities. Based on these data, we created a column-line composite chart as shown in Fig. 10.

Fig. 10 shows that the maximum equivalent stress experienced by the passenger car onboard hydrogen storage system exceeds that of the commercial vehicle system. Under the Psd4 road condition, the passenger car system experiences the highest equivalent stress across all directions, with a total stress of 347.31 MPa. However, the maximum deformation occurs under the Psd6 condition, measuring 4.1898 mm. In contrast, the commercial vehicle system also experiences the highest stress and deformation under the Psd6 condition, with an equivalent stress of 134.77 MPa and a deformation of 6.2385 mm. Comparative analysis reveals that the vibration spectrum of road condition 6 has the most significant impact on the failure potential of the onboard hydrogen storage system, making it more prone to failure under this condition. Furthermore, the random vibration simulation results show a clear correlation between equivalent stress and deformation: as the equivalent stress increases, so does the deformation.

The analysis of vibration-induced failures in onboard hydrogen

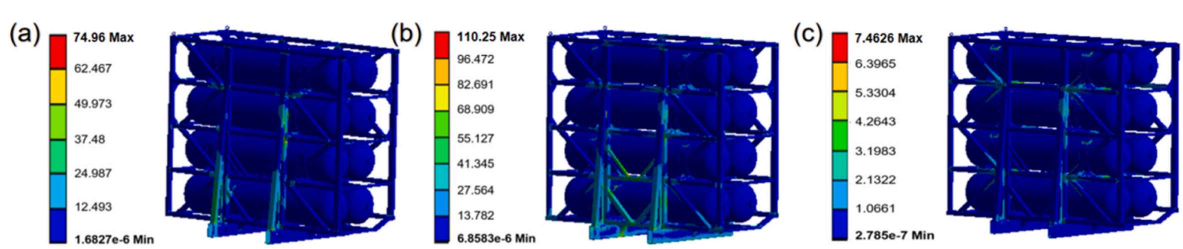

Fig. 8. Equivalent stress contours of random vibration for commercial vehicle onboard hydrogen storage system: (a) X-direction; (b) Y-direction; (c) Z-direction.

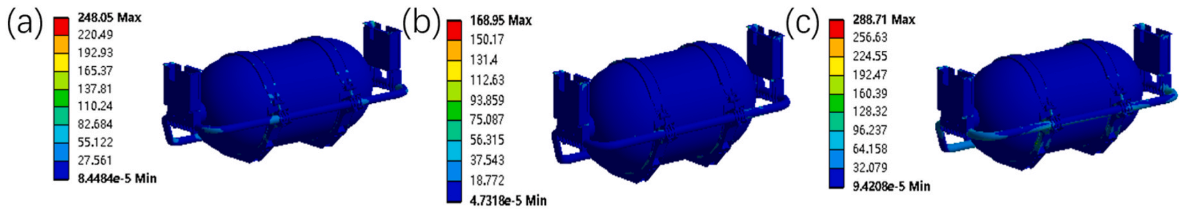

Fig. 9. Equivalent stress contour of random vibration for passenger vehicle onboard hydrogen storage system: (a) X-direction; (b) Y-direction; (c) Z-direction.

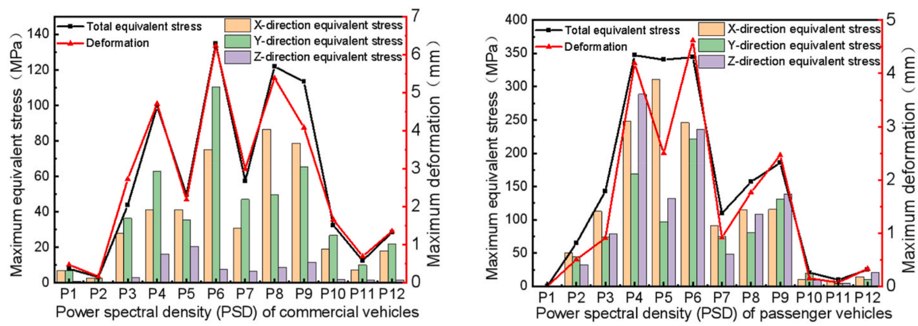

Fig. 10. Random vibration simulation results of onboard hydrogen storage systems: (a) commercial vehicle configuration, (b) passenger vehicle configuration. 'p' in the figure stands for PSD.

storage systems reveals two distinct failure mechanisms: “resonance phenomenon [45]" and “vibration fatigue [46]".

The resonance phenomenon arises when the excitation frequency of external vibration loads matches the natural frequency of the system. Under these conditions, all contacting components experience additional dynamic stresses. As vibrations persist, these stresses gradually enlarge inter-component clearances and disrupt contact pressure distribution. When pressure falls below critical thresholds, instantaneous constraint loss occurs, potentially leading to sudden fracture failure. This failure risk increases proportionally with both number and amplitude of vibrations - higher frequency and greater vibration magnitude significantly raise the probability of failure. Conversely, vibration fatigue results from prolonged exposure to irregular vibrations. In this process, cyclic stress loading gradually builds up stress concentration in the system. When these concentrated stresses exceed the yield limit of the material, fatigue cracks begin to form. Continued cyclic stresses then propagate these cracks until they reach critical size, ultimately causing structural failure at stress concentration areas. This mechanism exhibits the characteristic progressive degradation pattern typical of fatigue failures.

4. Conclusion

This study presents a comprehensive investigation into the failure mechanisms of onboard hydrogen storage systems by collecting multi-dimensional acceleration signals from 12 representative road conditions through real-world vehicle testing. After signal processing and transformation into vibration spectrum data, random vibration simulations were performed on hydrogen storage systems. Modal analysis results, together with the RMS values of the power spectral density signals, were utilized to evaluate system responses and identify failure modes and characteristics. The key findings are summarized as follows.

(1) Under identical road conditions, passenger vehicle hydrogen storage systems exhibit stronger vibrational responses compared to those in commercial vehicles. This is primarily attributed to the design priorities of passenger vehicles, which emphasize ride comfort, resulting in higher vibration transmission. In contrast, commercial vehicles employ more rigid structural layouts that effectively dampen vibrational energy.

(2) Stress concentration regions were identified under specific road conditions—condition 6 for commercial vehicles and condition 4 for passenger vehicles—where the systems experienced maximum equivalent stresses of 134.77 MPa and 344.45 MPa, respectively. Structural components such as the cylinder saddle and support brackets were prone to deformation and fracture, leading to connection loosening, structural collapse, and potential detachment of the hydrogen cylinders. Notably, road condition PSD6 was found to be particularly detrimental due to its ability to simultaneously induce peak stress and deformation, thereby amplifying the risk of compound structural failure.

(3) The primary failure mechanisms were identified as resonance and vibration-induced fatigue. Resonance occurs when external excitation frequencies align with the natural frequencies of the system, generating excessive dynamic stresses that enlarge clearances between components and ultimately lead to material failure. In parallel, continuous exposure to high-frequency vibrations initiates fatigue processes, characterized by localized stress concentration, crack initiation, and eventual propagation to critical failure—particularly at bracket connections.

These findings offer valuable insights into the structural optimization and failure prevention of onboard hydrogen storage systems, contributing to the design of safer hydrogen-powered vehicles.

CRediT authorship contribution statement

Tao Zhang: Writing – original draft. **Zhijie Duan:** Resources, Conceptualization. **Feiyang Liu:** Supervision, Resources, Methodology, Data curation. **Weijie Yang:** Writing – review & editing, Resources.

Declaration of competing interest

Data are available upon request from the authors.

Acknowledgments

This work was funded by the Natural Science Foundation of Hebei (E2020502023) and Key R&D Project under China's 14th Five-Year Plan: Safety Assessment Technologies and Equipment for Onboard Energy Storage Systems in New Energy Vehicles (Project No. 2021YFB2501500).

References

[1] Shen Y, Lv H, Hu Y, et al. Preliminary hazard identification for qualitative risk assessment on onboard hydrogen storage and supply systems of hydrogen fuel cell vehicles. Renew Energy 2023;212:834–54.
[2] Mulky L, Srivastava S, Lakshmi T, et al. An overview of hydrogen storage technologies – key challenges and opportunities. Mater Chem Phys 2024;325:129710.
[3] Liu Y-L, Zhao Y-Z, Zhao L, et al. Experimental studies on temperature rise within a hydrogen cylinder during refueling. Int J Hydrogen Energy 2010;35(7):2627–32.
[4] Wang L, Zheng C, Wei S, et al. Thermo-mechanical investigation of composite high-pressure hydrogen storage cylinder during fast filling. Int J Hydrogen Energy 2015;40(21):6853–9.
[5] Galassi MC, Baraldi D, Acosta Iborra B, et al. CFD analysis of fast filling scenarios for 70 MPa hydrogen type IV tanks. Int J Hydrogen Energy 2012;37(8):6886–92.
[6] Zhou W, Wang J, Pan Z-B, et al. Review on optimization design, failure analysis and non-destructive testing of composite hydrogen storage vessel. Int J Hydrogen Energy 2022;47(91):38862–83.
[7] Zhang Y, Gu J, Pan S, et al. Numerical study on the influence of liner geometry and lay-up sequence on the fatigue life of composite hydrogen storage vessel. Int J Pres Ves Pip 2023;205:104986.
[8] Liu Y, Wu X, Liu K, et al. An investigation into vibration-induced fatigue failure of metro vehicle cowcatcher and its structural improvement design. Eng Fail Anal 2023;145:107038.
[9] Wu X, Xie C, Liu K, et al. Study on high frequency vibration-induced fatigue failure of antenna beam in a metro bogie. Eng Fail Anal 2022;133:105976.
[10] Lee J, Kim S. Effect of operation conditions on the structural and fatigue behaviors of hydrogen storage vessel in refueling station. Int J Hydrogen Energy 2025;97:469–82.
[11] Lei W, Jiang Y, Zhou X, et al. Vibration fatigue analysis of structures under non-stationary and non-gaussian random excitation. Probab Eng Mech 2025;79:103744.
[12] Kinoshita T, Okamura S, Nishino H, et al. Vibration test and fatigue test for failure probability evaluation method with integrated energy. Int J Pres Ves Pip 2024;211:105299.
[13] Manouchehrynia R, Abdullah S, Singh SSK. Fatigue-based reliability in assessing the failure of an automobile coil spring under random vibration loadings. Eng Fail Anal 2022;131:105808.
[14] Chen YS, Wang CS, Yang YJ. Combining vibration test with finite element analysis for the fatigue life estimation of PBGA components. Microelectron Reliab 2008;48(4):638–44.
[15] Wang Y, Li S, Wei N. Dynamic response impact of vehicle braking on simply supported beam bridges with corrugated steel webs based on vehicle-bridge coupled vibration analysis. CMES - Computer Modeling in Engineering and Sciences 2024;139(3):3467–93.
[16] Zhang P, Yu Z. Random vibration analysis of the maglev vehicle-guideway system using a probability density evolution method with uncertain parameters. Structures 2023;48:346–59.
[17] You T, Zhou J, Gong D, et al. Synthesis of random vibration environment spectra for the fatigue analysis and optimization of railway vehicles. Int J Fatig 2022;159:106752.
[18] Wang Q, Zhao Y. Vibration reduction research of a thin beam system by employing distributed coupling nonlinear energy sinks. Chaos Solitons Fractals 2025;192:116047.
[19] Aathif Akmal SM, Bharathiraja G. Analysis of engine mount material for automotive vibration and noise reduction. Mater Today Proc 2022;62:2235–9.
[20] GonzáLEZ A, Feng K, Casero M. Effective separation of vehicle, road and bridge information from drive-by acceleration data via the power spectral density resulting from crossings at various speeds. Developments in the Built Environment 2023;14:100162.
[21] Yin T, Yuen K-V, Zhu H-P. A novel Bayesian framework for time-domain operational multi-setup modal analysis: theory and parallelization. Eng Struct 2025;322:119167.
[22] Dethof F, KeßLER S. Explaining impact echo geometry effects using modal analysis theory and numerical simulations. NDT E Int 2024;143:103035.
[23] Liu Z, Zhang X, Wang K-W, et al. Data-driven modeling of multi-stable origami structures: extracting the global governing equation and exploring the complex dynamics. Mech Syst Signal Process 2024;220:111659.
[24] Mackie G, Pacheco A, Sequeira C. Application of simple harmonic motion theory to the prediction of floating wind turbine first order motions. Ocean Eng 2023;271:113710.
[25] Tsai T-Y, Yeh C-L, Lai Y-S, et al. Response spectra analysis for undamped structural systems subjected to half-sine impact acceleration pulses. Microelectron Reliab 2007;47(8):1239–45.
[26] Liang W, Liang M, Chen R, et al. Dynamic responses of undamped oscillator subjected to underwater shock wave. Int J Mech Sci 2025;289:110094.
[27] De Carolis S, Messina A, Soria L. Modal analysis through response-based FRFs: additional modes for local diagnoses. J Sound Vib 2023;549:117574.
[28] Xie Z, Yang K, Yang M, et al. The anti-random impact performances of a novel propulsive bearing-shaft system: theory and experiment. Mech Syst Signal Process 2025;225:112309.
[29] Hariri-Ardebili MA, Mahdi Seyed-Kolbadi S, Saouma VE, et al. Anatomy of the vibration characteristics in old arch dams by random field theory. Eng Struct 2019;179:460–75.
[30] de Miguel N, Acosta B, Moretto P, et al. The effect of defueling rate on the temperature evolution of on-board hydrogen tanks. Int J Hydrogen Energy 2015;40(42):14768–74.
[31] DenoëL V. On the background and biresonant components of the random response of single degree-of-freedom systems under non-Gaussian random loading. Eng Struct 2011;33(8):2271–83.
[32] Zhou R, He M, Cai J, et al. Non-stationary buffeting responses of a twin-box girder suspension bridge with various evolutionary spectra. Probab Eng Mech 2024;76:103625.
[33] Zhang H, Zhao Y-G. Damping modification factor based on random vibration theory using a source-based ground-motion model. Soil Dynam Earthq Eng 2020;136:106225.
[34] Li Y, Dave AJ, Elmer TW, et al. Numerical analysis with experimental validation of tube fatigue failure in feedwater heaters. Eng Fail Anal 2025;181:109990.
[35] Abdullah L, Singh SSK, Abdullah S, et al. Fatigue reliability and hazard assessment of road load strain data for determining the fatigue life characteristics. Eng Fail Anal 2021;123:105314.
[36] Zhao J, Wong PK, Ma X, et al. Simplification of finite element modeling for plates structures with constrained layer damping by using single-layer equivalent material properties. Compos B Eng 2019;157:283–8.
[37] Huang JH. Vibration and shock analysis of the hydrogen supply 43ystem for fuel cell vehicles and frame size optimization [D]. Beijing University of Chemical Technology; 2019. https://doi.org/10.26939/d.cnki.gbhgu.2019.000909.
[38] Li J, Zhang X, Song H. Understanding self-excited vibration mechanism with modal analysis theory. Mech Syst Signal Process 2025;230:112576.
[39] Katam R, Polepally G, Pasupuleti VDK, et al. Assessment of damage location and its severity using modal analysis: insights from analytical, numerical, and experimental approaches. Structures 2025;71:108062.
[40] Zhang B, Tan CA, Dai T. Ride comfort and energy dissipation of vehicle suspension system under non-stationary random road excitation. J Sound Vib 2021;511:116347.
[41] Manouchehrynia R, Abdullah S, Singh SSK, et al. Reliability-based fatigue life assessment using random road load condition and local damage criteria. Eng Fail Anal 2023;146:107157.
[42] Wang A, Wang H, Ling C, et al. Fatigue life prediction of rubber suspension bushings based on virtual road load spectrum pulses. Results Eng 2024;23:102693.
[43] Semmlow J. Chapter 3 - signal analysis in the frequency domain: the Fourier series and the Fourier transformation [M]//SEMMLOW J. Circuits, Signals, and Systems for Bioengineers. fourth ed. Academic Press; 2025. p. 119–79.
[44] Ye Q, Jia Z-Z, Liu W, et al. Numerical simulation on destruction process of ventilation door by gas explosion. Procedia Eng 2018;211:934–44.
[45] Hao Y, Shou X, Yu X. Stochastic resonance phenomenon of shape memory alloy strip plates under main resonance. Int J Non Lin Mech 2025;171:105020.
[46] Safaeinejad A, Rahimi M, Zhou D, et al. A sensorless active control approach to mitigate fatigue loads arising from the torsional and blade edgewise vibrations in PMSG-based wind turbine system. Int J Electr Power Energy Syst 2024;155:109525.